mate agreement with the gallium arsenide band structure calculated by Bassani and Yoshimine,[3] but yields the result that Γ_1 lies below Γ_{15}. This appears to be in better agreement with experimental evidence, such as piezoresistance and magnetoresistance measurements, which seem to indicate that the bottom of the conduction band is at Γ_1. The band gap was found to be of the same order of magnitude as that found experimentally.

I wish to express my gratitude to Professor E. Brown for his guidance and encouragement throughout the completion of this work. I further wish to acknowledge that most of the computations were performed at the Rensselaer Polytechnic Institute Computer Laboratory.

[3] F. Bassani and M. Yoshimine, Phys. Rev. **130**, 20 (1963).

PHYSICAL REVIEW VOLUME 135, NUMBER 2A 20 JULY 1964

Spectral Shape and Attenuation Length for Hot Electrons in the Presence of Finite Absorption

G. A. BARAFF
Bell Telephone Laboratories, Murray Hill, New Jersey
(Received 2 March 1964)

The space and energy distribution of electrons released into a field-free semiconductor provides a means of studying the interaction of the electrons with the material, as experiments by Bartelink, Moll, and Meyer have shown. In the presence of finite absorption, or large energy losses per collision, the conventional methods of solving the Boltzmann equation governing the distribution function fail to give reliable results. We have found that a considerable amount of information may be obtained from the Boltzmann equation itself without a spherical harmonic expansion by studying its Laplace transform with respect to energy. In particular, we obtain an analytic expression for the exponential attenuation length which reduces to the BMM expression in the limit of small absorption and small energy loss. We obtain expressions for the average energy loss and average spread of the distribution, both of which increase linearly with distance, and for the total intensity of the distribution, which decreases exponentially with the distance through which the electrons must diffuse. This form of variation is independent of the energy distribution of the source of hot electrons. Therefore, if the energy distribution of electrons is measured at two different distances from the same source, the rate at which the average energy, for example, decreases with distance may be determined. This rate, being independent of the source distribution, is a characteristic of the medium, as is the BMM attenuation length. These two quantities together provide sufficient information to determine the mean free path for optical phonon emission and the mean free path for impact ionization. Measuring the energy distribution of the electrons in the medium can be done by measuring the distribution of electrons emitted into the vacuum provided that the angular distribution of the particles is known. This angular distribution may be approximated from knowledge of the Laplace transform. The effect of this analysis on the interpretation of the BMM experiments is to suggest that the mean free path for impact ionization in silicon may be closer to 300 Å than to 200 Å.

I. INTRODUCTION

THE space and energy distribution of particles released into a field-free medium by a high-energy localized source provides a means of studying the interaction of the particles with the medium. A recent example of this technique is to be found in a paper by Bartelink, Moll, and Meyer dealing with the emission of hot electrons from shallow $p-n$ junctions in silicon.[1] In the experiments reported in the BMM paper, electrons in the silicon are accelerated by an electric field and are then allowed to diffuse through a field-free region in which they may either lose energy or—in effect—be absorbed. Other examples may be found among the problems faced by the designers and users of nuclear reactors.[2] Here, the particles of interest are neutrons, and not surprisingly, a substantial part of neutron transport theory is concerned with the calculation of just this space- and energy-dependent distribution function.[3]

The similarities between the hot electron problem of the BMM experiment and the neutron diffusion problem are so great that it was virtually inevitable that BMM should have employed one of the most useful of the approximations developed by the neutron transport workers—the Fermi age theory[2–4]—in the analysis of their experiments. The hot electron problem is, however, sufficiently simpler than the neutron diffusion problem that it is possible to obtain much exact information about the distribution without making the age theory approximation. This is important because, although the age theory is known to be valid in the limit of infinitesimal absorption and infinitesimal energy loss per collision, its validity for the finite absorptions and finite

[1] D. J. Bartelink, J. L. Moll, and N. I. Meyer, Phys. Rev. **130**, 972 (1963). The authors and this reference will be denoted BMM.
[2] R. L. Murray, *Nuclear Reactor Physics* (Prentice Hall, Inc., Englewood Cliffs, New Jersey, 1957).
[3] B. Davison, *Neutron Transport Theory* (Clarendon Press, Oxford, 1957).
[4] S. Glasstone and M. C. Edlund, *The Elements of Nuclear Reactor Theory* (D. Van Nostrand and Company, Inc., Princeton, New Jersey, 1952).

energy losses of physical interest in the hot electron problem has not been adequately examined.

The simplicity of the hot electron problem resides in the primitive nature of the model used to describe the transport of the hot electrons in semiconductors. In this model which has been used by many workers,[5–7] electron-electron interaction is neglected and the interaction of the electron with the medium is characterized by three parameters: l_r the mean free path for the electrons to cause emission of an optical phonon, $\mathcal{E}_r$ the energy of that phonon, and l_i the mean free path for the electron to cause impact ionization. The process of phonon emission is treated as an isotropic scattering event in which the electron loses the energy $\mathcal{E}_r$; the process of ionization is treated as a scattering in which the electron loses so much energy that it is removed from the distribution in the energy range of interest, i.e., ionization is treated as an absorption.

The purpose of the present work is to extract a certain amount of exact information from the model *without* making the age approximation. In particular, the attenuation length and the low-order spectral moments (to be defined subsequently) are quantities which may be calculated analytically. From these moments, one can compute the total intensity, average energy, and average spread of the distribution. These three parameters are especially useful in describing the distribution for the following reason: The change in these quantities produced by altering the thickness of material through which the electrons must travel will turn out to be completely independent of the mechanism by which the electrons are heated. Hence, if the emerging spectrum is measured for two different thicknesses of material, one can, with no knowledge of threshold for ionization or the field distribution which accelerated the electrons, obtain three numbers which depend on l_i, l_r, and $\mathcal{E}_r$ only. These three numbers, and the exponential attenuation length L_0 (a fourth function of l_i, l_r, and $\mathcal{E}_r$) are more than adequate to determine l_i and l_r. Moreover, these three parameters are very nearly sufficient, as will be shown, to describe the entire shape of the spectrum.

The second section of this paper is meant to be a mathematical introduction and outline. In that section will be found the definition of the attenuation length, spectral moments, average energy, and average spread. These quantities are all related to the Laplace transform of the collision density, which is the key element in the calculation scheme to follow. The mathematics used in that section will be simple, general, and will contain ideas developed in the succeeding sections. The attenuation length is calculated in Sec. III. Spectral moments and averages are calculated in Sec. IV by two methods, one which is useful provided that the source is not too near, and the other, by the age theory approximation. Results are presented in the form of graphs; the analytic expressions being plotted will be found in the appendix.

Although it is possible to invert the Laplace transformation when the age approximation is used, inversion of the transform of the exact collision density has not been accomplished. Because there is some advantage in having a function to contemplate rather than some numbers (the moments) which describe it, we introduce in Sec. II a simple trial function which, with parameters adjusted to give the age approximate moments, accurately reproduces the age approximate collision density. This same function, with parameters adjusted to give the exact moments, should reproduce the exact collision density as well. Use of this trial function makes possible a calculation of the angular distribution and current in Sec. V. The current turns out to be related to the density gradient in a way which closely resembles the ordinary Fick's law of diffusion but with differences which arise because of the finite absorption and the finite energy loss.

The main reason for interest in the angular distribution is its relation to the current of particles actually emitted from the medium, the quantity studied in the BMM experiments. A calculation of the emitted current concludes Sec. V. Finally, Sec. VI contains a discussion of the effect of this work on the interpretation of the BMM experiments.

II. GENERAL FEATURES OF THE DISTRIBUTION

The exponential attentuation of a flux of particles is a characteristic of the bulk properties of the material and does not depend on the details of the process by which the particles are introduced or removed from the material through which they must pass. For this reason, the exponential attenuation length can be calculated by solving an infinite medium problem, a much simpler task than is solving one in which surface conditions must be specified. The appropriate infinite medium problem is, of course, one in which the distribution depends on a single spatial coordinate, say, on x only. The source of particles may then be placed on the plane $x=0$.

The details of the distribution near a boundary far from the source may be of interest. Suppose that the medium is field free and semi-infinite, the boundary boundary being at $x=L$, and suppose that all particles which reach the boundary are emitted. This boundary condition may be shown to be very nearly equivalent to demanding that the particle density go to zero along some plane $x=L'$, where L and L' are within one mean free path of each other.[8] The distribution whose density vanishes along the plane $x=L'$ can always be constructed from the infinite medium distribution by the method of images; that is, one subtracts from the infinite medium distribution with source at $x=0$ another infinite medium distribution whose source is at $x=2L'$. Since

[5] P. A. Wolff, Phys. Rev. **95**, 1415 (1954).
[6] W. Shockley, Solid State Electron. **2**, 35 (1961).
[7] J. L. Moll and R. Van Overstraeten, Solid State Electron. **6**, 147 (1963).

[8] P. M. Morse and H. Feshbach, *Methods of Mathematical Physics* (McGraw-Hill Book Company, Inc., New York, 1953). See their Eq. (2.4.34) and their Fig. 2.20.

each density is symmetric about its own source, the difference vanishes halfway between the two sources, at $x=L'$. A related method of images can also be used if the boundary at L is totally reflecting. Thus, the physics of the semi-infinite medium problem is largely contained in the solution to the infinite medium problem.

Suppose now that there is a spherically symmetric source of monoenergetic electrons of energy E_0 located along the plane $x=0$. The resulting distribution function will be denoted $f(x,\mathbf{p};E_0)$, where $\mathbf{p}$ is the momentum. It is convenient to work, not with f, but with a collision density $Q(x,E;E_0)$, equal to the rate at which electrons of energy E suffer collisions in a unit volume at x. If the mean free time for collisions of all types is denoted by $\tau(\mathbf{p})$, then the collision density can be found by integrating f/τ over all momenta whose energy $E(\mathbf{p})$ is equal to E.

$$Q(x,E;E_0)=\int d\mathbf{p}\delta[E-E(\mathbf{p})]f(x,\mathbf{p},E_0)/\tau(\mathbf{p}). \quad (2.1)$$

If the electrons at $x=0$ are released, not just at energy E_0 but in a distributed source $S(E_0)$, then the collision density M at the plane x will be given by integrating Q over the source

$$M(x,E)=\int_0^\infty Q(x,E;E_0)dE_0S(E_0). \quad (2.2)$$

There is no way that an electron can increase its energy in the model described in Sec. I. Hence, an electron released at energy E_0 can contribute to a collision density at energy E only if $E<E_0$, i.e., Q vanishes if $E>E_0$. Because the parameters of the model are independent of energy, the probability that an electron loses an energy $U=E_0-E$ [suffers $(E_0-E)/\mathcal{E}_r$ collisions] in diffusing a distance x will depend on the energy loss E_0-E rather than on E and E_0 separately. From this it follows that

$$Q(x,E;E_0)=q(x,E_0-E)\equiv q(x,U), \quad (2.3a)$$

$$q(x,U)=0 \quad \text{if} \quad U<0, \quad (2.3b)$$

so that

$$M(x,E)=\int_E^\infty q(x,E_0-E)dE_0S(E_0). \quad (2.4)$$

This relation between source spectrum S and collision density M has some very useful consequences. The first is that an exponential source with temperature kT_e

$$S(E_0)=\exp(-E_0/kT_e)$$

gives rise to an exponential collision density

$$M(x,E)=e^{-E/kT_e}\int_0^\infty q(x,U)e^{-U/kT_e}dU. \quad (2.5)$$

This exponential collision density has the same temperature as the source and a spatial dependence (the integral above) which is just the Laplace transform of q,

$$q_s(x)\equiv\int_0^\infty q(x,U)e^{-sU}dU, \quad (2.6)$$

with the transform variable s set equal to the reciprocal temperature. It will turn out that this integral has a spatial dependence $\exp(-x/L_0)$, and this then defines the attenuation length L_0.

The second consequence is the relationship between the total source strength S_0 for an arbitrary source distribution $S(E_0)$, and the total collision density $M_0(x)$ along the plane x. The total source strength and collision density are

$$S_0\equiv\int_0^\infty S(E_0)dE_0, \quad (2.7a)$$

$$M_0(x)\equiv\int_0^\infty M(x,E)dE. \quad (2.7b)$$

Integrating (2.4) over E, reversing the order of integration and substituting $U=E_0-E$ as the variable of integration gives the following relation between them:

$$M_0(x)=\int_0^\infty dE\int_0^\infty q(x,E_0-E)S(E_0)dE_0$$

$$=S_0Q_0(x), \quad (2.8)$$

where

$$Q_0(x)=\int_0^\infty q(x,U)dU. \quad (2.9)$$

The quantities S_0, M_0, and Q_0 are special examples of spectral moments which will be defined in general by

$$S_n\equiv\int_0^\infty S(E_0)E_0^ndE_0, \quad (2.10a)$$

$$M_n(x)\equiv\int_0^\infty M(x,E)E^ndE, \quad (2.10b)$$

$$Q_n(x)=\int_0^\infty q(x,U)U^ndU. \quad (2.10c)$$

These moments are useful quantities for describing the distributions $S(E_0)$ and $M(x,E)$. For instance, the average energy $\langle E_0\rangle$ of the source electrons and the average energy $\langle E(x)\rangle$ at which electrons collide on the plane at x are given by

$$\langle E_0\rangle\equiv\int_0^\infty S(E_0)E_0dE_0\Big/\int_0^\infty S(E_0)dE_0=S_1/S_0, \quad (2.11a)$$

$$\langle E(x)\rangle\equiv\int_0^\infty M(x,E)EdE\Big/\int_0^\infty M(x,E)dE$$

$$=M_1(x)/M_0(x). \quad (2.11b)$$

The average square deviation of the source from its average and the average square deviation of the collision density from *its* average are also expressible in terms of the moments

$$\delta_S^2 \equiv \langle E_0^2\rangle - \langle E_0\rangle^2 = S_2/S_0 - (S_1/S_0)^2, \tag{2.12a}$$

$$\delta_M^2(x) \equiv \langle E^2(x)\rangle - \langle E(x)\rangle^2 = M_2(x)/M_0(x) - [M_1(x)/M_0(x)]^2. \tag{2.12b}$$

The relation between the average energy of the source and of the collision density at x may we obtained by multiplying Eq. (2.4) by E, integrating over all E and dividing the result by Eq. (2.8). The relationship resulting is

$$\langle E(x)\rangle = \langle E_0\rangle - \langle U(x)\rangle, \tag{2.13a}$$

$$\langle U(x)\rangle = Q_1(x)/Q_0(x). \tag{2.13b}$$

The quantity $\langle U(x)\rangle$ defined by Eq. (2.13b) is obviously the average energy loss of those electrons which collide at the plane x. Therefore, Eq. (2.13a) states simply that the average energy at which electrons collide on the plane x is equal to this average energy of the source minus thier average energy loss in traversing the region from source to collision. This result might have appeared intuitively obvious: not so intuitive perhaps is the fact that the square deviations are also additive. One may verify, by multiplying Eq. (2.4) by E^2 and integrating, that

$$\delta_M^2(x) = \delta_S^2 + \delta_Q^2(x), \tag{2.14a}$$

$$\delta_Q^2(x) \equiv Q_2(x)/Q_0(x) - [Q_1(x)/Q_0(x)]^2. \tag{2.14b}$$

That is, any spread in the source distribution is augmented by adding the spread caused by transport of the electrons from source to collision.

The three parameters $M_0(x)$, $\langle E(x)\rangle$, and $\delta_M^2(x)$ contain quite a bit of information about the distribution $M(x,E)$ and hence can be used to characterize the distribution as well as can, say, the energy and magnitude of the peak of the distribution. These parameters have in addition the considerable advantage of a very simple spatial dependence. This will be confirmed in detail in later sections. It will turn out that at distances large compared to one mean free paths,

$$Q_0(x) = A\,\exp(-Bx/l), \tag{2.15a}$$

$$\langle U(x)\rangle = \mathcal{E}_r(C+Dx/l), \tag{2.15b}$$

$$\delta_Q^2(x) = \mathcal{E}_r^2(F+Gx/l), \tag{2.15c}$$

where l is the total mean free path and the six constants A, B, C, D, F, G depend only on r, the ratio of mean free paths

$$r = l_i/l_r. \tag{2.16}$$

Therefore, if the parameters S_0, $\langle E_0\rangle$, and δ_S^2 describing an arbitrary source are given, then the parameters describing the collision density will be, using (2.8), (2.13), (2.14), and (2.15)

$$M_0(x) = S_0 A\,\exp(-Bx/l), \tag{2.17a}$$

$$\langle E(x)\rangle = \langle E_0\rangle - \mathcal{E}_r(C+Dx/l), \tag{2.17b}$$

$$\delta_M^2(x) = \delta_S^2 + \mathcal{E}_r^2(F+Gx/l). \tag{2.17c}$$

If, on the other hand, the source parameters are not known, then observation of the collision density at two values of x, say x_1 and x_2, and computation of the parameters from the observed distribution gives

$$B/l = (x_2-x_1)^{-1}\ln[M_0(x_0)/M_0(x_1)], \tag{2.18a}$$

$$D\mathcal{E}_r/l = (x_2-x_1)^{-1}[\langle E(x_0)\rangle - \langle E(x_1)\rangle], \tag{2.18b}$$

$$G\mathcal{E}_r^2/l = (x_2-x_1)^{-1}[\delta_M^2(x_2) - \delta_M^2(x_1)], \tag{2.18c}$$

i.e., three numbers which are independent of the source distribution $S(E_0)$, and which may be used to determine l_i and l_r.

The three moments Q_0, Q_1, and Q_2 which alone are needed for calculation of the six constants in Eq. (2.15) may be obtained directly from the Laplace transform (2.6) without ever performing the inversion. One need only differentiate the transform n times with respect to s and then set s equal to zero

$$\lim_{s\to 0}\left(-\frac{d}{ds}\right)^n q_s(x) = \int_0^\infty q(x,U)U^n dU = Q_n(x). \tag{2.19}$$

Thus, the transform $q_s(x)$ supplies both the attenuation length L_0 and the six constants.

The reason for all this emphasis on quantities which can be calculated from the Laplace transform $q_s(x)$ without knowing the distribution $q(x,U)$ is, of course, that we are unable to calculate $q(x,U)$ even though we do know the transform $q_s(x)$ exactly. Our knowledge of $q_s(x)$ arises in an interesting way: In the first section of this paper we stressed the analogy between the hot electron problem and the neutron diffusion problem; that analogy appears once again, for now, it turns out that the transform $q_s(x)$ is exactly the density function in *monoenergetic* neutron diffusion theory.[3,9] This density function is well known and so we can again draw on some of the exact results of neutron transport theory to solve the hot electron problem.

Our inability to calculate $q(x,U)$ from $q_s(x)$ is not as serious a difficulty as one might anticipate because quite a bit is already known about the qualitative behavior of $q(x,U)$. The qualitative information about $q(x,U)$ is the following:

(a) It is nonnegative because of its definition.

(b) It probably has a single maximum, because of the physical arguments presented so clearly by BMM.

(c) Its dependence on U at large U will be exponentially decreasing because each collision which increases

[9] K. M. Case, F. de Hoffman, and G. Placzek, *Introduction to the Theory of Neutron Diffusion* (U. S. Government Printing Office, Washington, D. C., 1953).

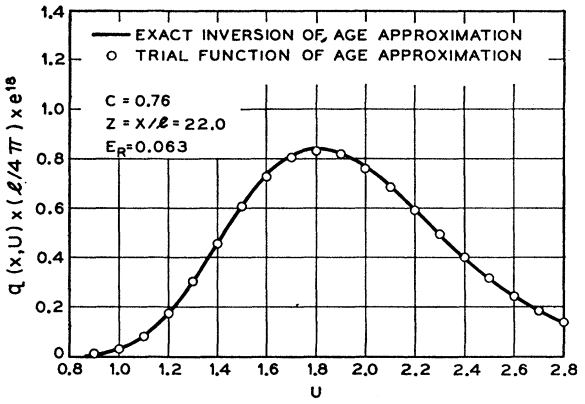

FIG. 1. Comparison of age distribution with its trial function approximant.

U by a constant *amount* $\mathcal{E}_r$ decreases the electron population by a constant *fraction* c_0, the probability that the electron survives a collision.

In addition to the qualitative information, the parameters Q_0, $\langle\bar{U}\rangle$ and $\delta_Q{}^2$ provide three pieces of quantitative information about $q(x,U)$ namely, its integral over U, its average U and its spread about that average. Taken together, the quantitative and qualitative information leave little freedom in the shape of $q(x,U)$ even though a variety of functional forms might successfully simulate this single shape.

A simple trial function which is consistent with the qualitative information is

$$q_n(x,U)=\alpha(U-U_0)^n\exp[-\gamma(U-U_0)],\quad U>U_0$$
$$=0,\qquad U<U_0. \tag{2.20}$$

Other trial functions come to mind but this one has the advantage that, for integer n, the moments can be easily calculated

$$Q_m(x)\equiv\int dU q_n(x,U)U^m.$$

Roughly speaking, one may think of the parameter α as adjusting the normalization, the parameter U_0 as shifting the distribution so as to adjust the average energy, and the parameters n and γ as adjusting the width of the distribution. One finds that

$$Q_0(x)=\alpha n!/\gamma^{n+1},$$
$$\bar{U}\equiv\langle U(x)\rangle\equiv Q_1/Q_0=U_0+(n+1)/\gamma, \tag{2.21}$$
$$\delta^2\equiv\delta_Q{}^2(x)\equiv Q_2/Q_0-(Q_1/Q_0)^2=(n+1)/\gamma^2.$$

The quantities on the left of (2.21) are known. Hence Eq. (2.21) may be solved for α, U_0, and γ.

$$\gamma=[(n+1)/\delta^2]^{1/2},$$
$$U_0=\bar{U}-[(n+1)\delta^2]^{1/2}, \tag{2.22}$$
$$\alpha=(Q_0/n!)[(n+1)/\delta^2]^{(n+1)/2}.$$

By choosing α, γ, and U_0 in this way, the trial function and the exact function agree qualitatively and, to the extent of our knowledge of the exact function, quantitatively.

Although the parameters on the left of (2.22) are highly dependent on the value chosen for n, the trial function itself is rather insensitive. A simple way to demonstrate this is to calculate the magnitude and position of the peak of the trial function. This calculation may be found in Appendix C. Also to be found in Appendix C are the considerations of the analytic properties of the Laplace transform of $q_n(x,U)$ which lead to a unique choice of n.

It is interesting to compare the shape of the trial function with the function which it is supposed to simulate. The age theory calculation described in Appendix B leads to an explicit $q(x,U)$ for which the trial function parameters can be calculated and for which the trial function can be evaluated. A comparison of the explicit $q(x,U)$ and of the trial function approximation to it appears as Fig. 1. There is no inherent reason that the same trial function calculated using the parameters (2.22) should fail to simulate the true collision density as well.

Thus, even without knowing how to invert the Laplace transform, we have obtained a function which probably provides a useful substitute for the real $q(x,U)$. The utility of this substitute will be more apparent in Sec. V when we use this collision density to calculate the angular distribution near the boundary of a semi-infinite medium so as to be able to apply the ideas just outlined to the analysis of the BMM experiments.

III. THE ATTENUATION LENGTH

In this section, we shall display the Boltzmann equation corresponding to the model of Sec. I, take the Laplace transform and, setting s equal to the reciprocal temperature, we shall calculate the attenuation length. The resulting expression will be shown, under the conditions for which the age approximation is valid, to reduce to the expression given by BMM.

The Boltzmann equation governing $f(x,p,E_0)$ of Sec. II is

$$\left[V_x\frac{\partial}{\partial x}+\frac{1}{\tau(\mathbf{p})}\right]f(x,\mathbf{p},E_0)$$
$$=\int d\mathbf{p}'F(\mathbf{p}\leftarrow\mathbf{p}')f(x,\mathbf{p}';E_0)$$
$$+\delta(x)\delta[E_0-E(\mathbf{p})]\Big/\int d\mathbf{p}'\delta[E_0-E(\mathbf{p}')]. \tag{3.1}$$

Here, $\tau(\mathbf{p})$ is the momentum-dependent mean free time for scattering of all types so that f/τ is the rate at which scattering removes electrons from the element $drd\mathbf{p}$. The collision recovery function $F(\mathbf{p}\leftarrow\mathbf{p}')$ describes the rate

at which particles with momentum $\mathbf{p}'$ are scattered back into this element. The last term in (3.1) is the source of monoenergetic electrons of energy E_0, located on the plane $x=0$.

The model described in Sec. I corresponds to the following choices:

$$E(\mathbf{p})=p^2/2m, \tag{3.2a}$$

$$\mathbf{V}=\partial E(\mathbf{p})/\partial\mathbf{p}=\mathbf{p}/m, \tag{3.2b}$$

$$1/\tau=p/ml, \tag{3.2c}$$

$$F(\mathbf{p}\leftarrow\mathbf{p}')=(4\pi p^2)^{-1}(p'/ml_r)\delta(p-p^*), \tag{3.2d}$$

$$p^*=[(p')^2-2m\mathcal{E}_r]^{1/2}. \tag{3.2e}$$

Here, m is the mass of the electron, p is the magnitude of $\mathbf{p}$ and the mean free path l is

$$1/l=1/l_i+1/l_r. \tag{3.2f}$$

As a result of these choices, the collision density Q of Eq. (2.1) is

$$Q(x,E;E_0)=(p^2/l)\int d\Omega f(x,\mathbf{p},E_0), \tag{3.3a}$$

where

$$d\mathbf{p}=p^2dpd\Omega, \tag{3.3b}$$

$$p=(2mE)^{1/2}. \tag{3.3c}$$

The momentum dependence of f will be a dependence only on the scalar p and on μ, the cosine of the angle between x and $\mathbf{p}$. It will be convenient to define

$$z=x/l, \tag{3.4a}$$

$$U=E_0-E, \tag{3.4b}$$

$$g(z,U,\mu)=(4\pi p^2/l)f(x,\mathbf{p};E_0), \tag{3.4c}$$

so that

$$Q(x,E;E_0)=\frac{1}{2}\int_{-1}^{1}d\mu g(z,U,\mu), \tag{3.5}$$

while g satisfies the equation derived from (3.1)

$$\left(\mu\frac{\partial}{\partial z}+1\right)g(z,U,\mu)$$

$$=\frac{c_0}{2}\int_{-1}^{1}d\mu' g(z,\,U-\mathcal{E}_r,\,\mu')+\frac{\delta(z)\delta(U)}{l}, \tag{3.6a}$$

$$c_0\equiv l/l_r. \tag{3.6b}$$

The quantity c_0 is the probability that an electron survives a given collision, i.e., emits a phonon, and ranges from zero to one. The ratio $r=l_i/l_r$ is, of course,

$$r=c_0/(1-c_0). \tag{3.7}$$

The dependence on E and E_0 separately has disappeared completely from Eq. (3.6), and hence, one may write

$$Q(x,E;E_0)\equiv q(z,U)=\frac{1}{2}\int_{-1}^{1}d\mu g(z,U,\mu). \tag{3.8}$$

The Laplace transform of Eq. (3.6) is

$$\left(\mu\frac{\partial}{\partial z}+1\right)g_s(z,\mu)=\frac{c}{2}\int_{-1}^{1}d\mu' g_s(z,\mu')+\frac{\delta(z)}{l}, \tag{3.9a}$$

where

$$g_s(z,\mu)\equiv\int_0^\infty g(z,U,\mu)e^{-sU}dU, \tag{3.9b}$$

$$c\equiv c(s)=c_0\exp(-s\mathcal{E}_r). \tag{3.9c}$$

Also, the transform of Eq. (3.8) is

$$g_s(z)=\frac{1}{2}\int_{-1}^{1}d\mu g_s(z,\mu). \tag{3.9d}$$

Note that the function $g_s(z)$ appearing in (3.9d) is just the Laplace transform of the collision density—the function $q_s(x)$ which plays the central role—expressed in terms of $z=x/l$.

For the purpose of calculating the exponential attenuation length, the hot electron distribution may be examined far from the source. Postulating that the spatial dependence will be exponential, one writes[10]

$$g_s(z,\mu)=h(\mu)\exp(-Kz) \tag{3.10}$$

inserts this into (3.9a), ignores the source and obtains

$$(-\mu K+1)h(\mu)=\frac{c}{2}\int_{-1}^{1}d\mu' h(\mu'). \tag{3.11}$$

Since the right-hand side of (3.11) is a constant independent of μ, the left-hand side is also a constant which may be set equal to unity. This means that

$$(-\mu K+1)h(\mu)=1$$

or

$$h(\mu)=(1-\mu K)^{-1}. \tag{3.12}$$

Inserting this solution back into both sides of (3.11) allows the integration to be carried out with the result

$$1=(c/K)\tanh^{-1}K. \tag{3.13}$$

Using (3.10) and (3.12) to evaluate (3.9d) gives

$$g_s(z)=\exp(-Kx/l)(1/K)\tanh^{-1}K$$

so that the exponential attenuation length is

$$L_0=l/K,$$

where K is the solution of (3.13) obtained, according to Eq. (2.5), by setting $s=1/kT_e$. Summarizing these results,

$$g_s(z,\mu)=(1-\mu K)^{-1}\exp(-Kz), \tag{3.14a}$$

$$L_0=l/K, \tag{3.14b}$$

$$K/c=\tanh^{-1}K, \tag{3.14c}$$

$$c=c_0\exp(-\mathcal{E}_r/kT_e). \tag{3.14d}$$

[10] This method of solution appears in Ref. 8, p. 1616 and Ref. 3, p. 53.

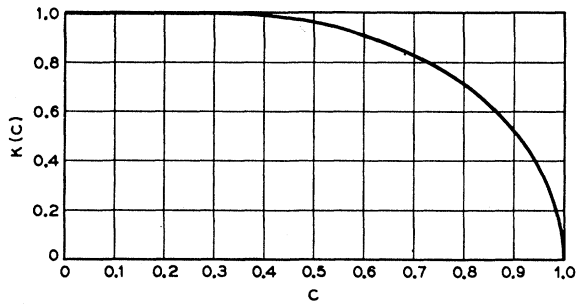

FIG. 2. The function $K(c)$: $(K/c)=\tanh^{-1}K$.

The function $K(c)$ defined by (3.14c) is well known in neutron transport work.[9] A numerical solution to (3.14c) may be obtained by two or three iterations of the equation

$$K=\tanh(K/c)$$

starting from an initial choice of $K=(3-3c)^{1/2}$. The values in Table I and graph (Fig. 2) have been taken from Ref. 9. Equation (3.14) is our exact expression for the exponential attenuation length.

The age theory approximation results when: (a) the distribution function is expanded in spherical harmonics and all but the first two are dropped, and; (b) the energy loss $\mathcal{E}_r$ is treated as infinitesimal. This was the technique used by BMM. To make contact with BMM, consider the spherical harmonics expansion of the angular dependence of (3.14a) namely,

$$(1-\mu K)^{-1}=\sum_{l=0}^{\infty} g_l(K)P_l(\mu). \tag{3.15}$$

A short calculation indicates that g_2/g_0 is proportional to K^2. Hence, the condition for the validity of the neglect of g_2 and higher terms is that K^2 be very small. Assuming that this is the case, one may expand (3.14c)

$$K/c\approx K+K^3/3$$

and solving for K, $K^2\approx 3(1-c)/c$. The smallness of K^2 then implies that c is very close to unity, so that one has

$$K^2\approx 3(1-c). \tag{3.16}$$

Treating $\mathcal{E}_r$ as small allows us to expand (3.14d) to lowest order to obtain

$$c=c_0(1-\mathcal{E}_r/kT_e). \tag{3.17}$$

Combining (3.14b), (3.16), and (3.17) gives

$$L_0^2=l^2/3[1-c_0(1-\mathcal{E}_r/kT_e)]$$

or, using definitions (3.2f), (3.6b), and (3.7),

$$L_0^2=ll_i/3[1+r\mathcal{E}_r/kT_e], \tag{3.18}$$

which is the formula given by BMM. Thus, the BMM formula which was obtained using age theory is indeed an approximation to the exact result (3.14). The approximation however, is valid only when C_0 is close to unity and $\mathcal{E}_r$ is small.

TABLE I. Numerical values of $K(c)$.

c	K	c	K	c	K
0.0	1.0000	0.5	0.9575	0.92	0.4740
0.1	1.0000	0.6	0.9073	0.94	0.4140
0.2	0.9999	0.8	0.8286	0.96	0.3408
0.3	0.9974	0.7	0.7104	0.98	0.2430
0.4	0.9856	0.9	0.5254	0.99	0.1725
				1.00	0.0000

IV. SPECTRAL MOMENTS AND AVERAGES

We now recognize that Eq. (3.9a) is precisely the Boltzmann equation which arises in monoenergetic neutron transport theory when neutrons suffer elastic collisions after being emitted from a plane source.[3,9] In the neutron work, the quantity c is the probability that the neutron survives the collision. In the hot electron problem, Eq. (3.9c) indicates that c is indeed proportional to c_0, the probability that the electron survives collision but here, c depends on the transform variable s as well. This is the only difference between the two problems and even this difference does not enter into the solution of Eq. (3.9a). We need only quote the solution to Eq. (3.9a) for $z>0$.[11]

$$lq_s(z)=\frac{1}{2}\int_0^1 \mu^{-1}g(c,\mu)\exp(-z/\mu)d\mu - (dK/dc)\exp(-Kz), \tag{4.1a}$$

where

$$1=(c/K)\tanh^{-1}K, \tag{4.1b}$$

$$g(c,\mu)=[(1-c\mu\tanh^{-1}\mu)^2+(\pi c\mu/2)^2]^{-1}. \tag{4.1c}$$

This solution (4.1a) consists of two terms, an integral and a term which, with different normalization, ap-

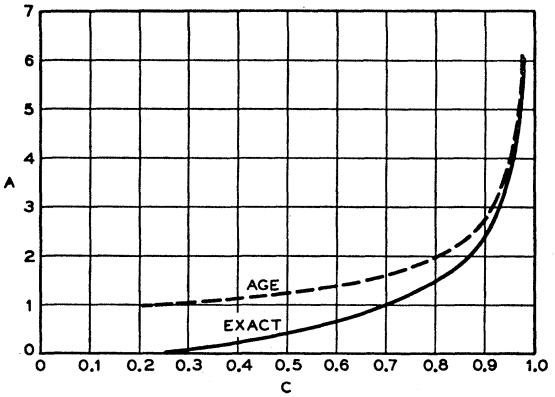

FIG. 3. The distribution constant A as a function of c.

[11] Reference 9, pp. 71 and 107.

TABLE II. The six constants as given by Eq. (A4).

c	lA	B	C	D	F	G
0.2	0.0045	1.0000	8.014	0.00090	−9.8889	0.00812
0.3	0.0583	0.9974	4.832	0.0175	−5.928	0.1021
0.4	0.1894	0.9856	3.479	0.0757	−3.535	0.3393
0.5	0.3822	0.9575	2.878	0.1911	−1.851	0.7412
0.6	0.6315	0.9073	2.679	0.3789	−0.2307	1.394
0.7	0.9594	0.8286	2.809	0.6716	2.256	2.558
0.8	1.444	0.7104	3.447	1.155	8.686	5.136
0.9	2.400	0.5254	5.806	2.160	43.91	14.70
0.92	2.761	0.4740	7.033	2.540	70.83	20.40
0.94	3.271	0.4140	9.039	3.080	129.5	31.08
0.96	4.120	0.3408	13.24	3.955	299.0	56.32
0.98	5.976	0.2430	25.72	5.857	1224	156.5
0.99	8.556	0.1725	50.71	8.471	4950	438.0

peared in the preceding section in which the presence of the source at $z=0$ was discounted. The second term on the right of Eq. (4.1a) will be designated the asymptotic solution because, as in the last section, it persists even at large distances from the source. The presence of the integral in (4.1a) is connected with the proximity of the source.

The exponential attenuation of the integral can be seen to be like $\exp(-z)$ while the attenuation of the asymptotic term is like $\exp(-Kz)$ with $K\leq 1$. At sufficiently large distance from the source, the integral becomes negligible with respect to the asymptotic term and may be discarded. The minimum distance at which this discard is permissible depends on $c(s)$, or since we shall soon set $s=0$, on c_0. The reader is referred to Ref. 9 for a fuller discussion of this point.

The moments may now be computed by differentiating the asymptotic solution with respect to s and then setting s equal to zero as in Eq. (2.19). In this connection, it is useful to note that the s dependence arises only through the dependence of $c(s)$ on s. Therefore, using Eq. (3.9c)

$$\frac{d}{ds}=\frac{dc}{ds}\frac{d}{dc}=c\mathcal{E}_r\frac{d}{dc}. \tag{4.2}$$

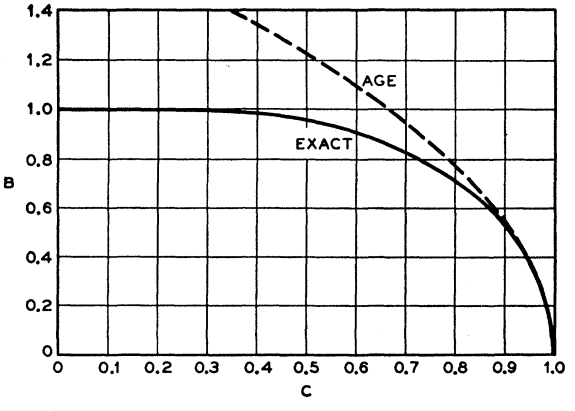

FIG. 4. The distribution constant B as a function of c.

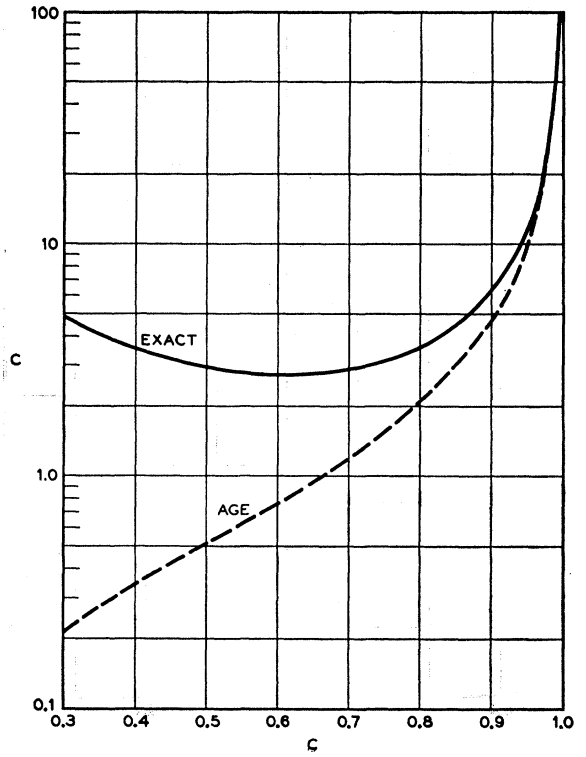

FIG. 5. The distribution constant C as a function of c.

The differentiations, construction of the average energy loss $\langle U(x)\rangle$ by Eq. (2.13b) and the construction of the average spread $\delta_Q^2(x)$ by Eq. (2.14b) are routine matters which offer no difficulty, and may be found in the Appendix A. The six constants $A\cdots G$ of Eq. (2.15) may be identified immediately and as promised, they depend only on the ratio of mean free paths. It is convenient to express them as functions of C_0. Table II lists the six constants and Figs. 3 through 8 display the same information in graphic form.

Also appearing in Figs. 3 through 8 are the values of the same six constants as calculated by age theory. The outlines of the age theory calculation may be found in

TABLE III. The six constants in the age approximation.

c	lA	B	C	D	F	G
0.2	0.9682	1.459	0.1250	0.1936	0.03125	0.0242
0.3	1.035	1.449	0.2143	0.3105	0.0918	0.0665
0.4	1.118	1.342	0.333	0.4472	0.2222	0.1491
0.5	1.225	1.225	0.5000	0.6124	0.5000	0.3062
0.6	1.369	1.095	0.7500	0.8216	1.125	0.6162
0.7	1.581	0.9487	1.167	1.107	2.722	1.291
0.8	1.936	0.7746	2.000	1.549	8.000	3.098
0.9	2.739	0.5477	4.500	2.465	40.50	11.09
0.92	3.062	0.4899	5.750	2.817	66.13	16.20
0.94	3.536	0.4240	7.833	3.323	122.7	26.03
0.96	4.333	0.3464	12.00	4.157	288.0	498.8
0.98	6.124	0.2449	24.50	6.001	1200	147.0
0.99	8.660	0.1732	49.50	8.574	4901	424.4

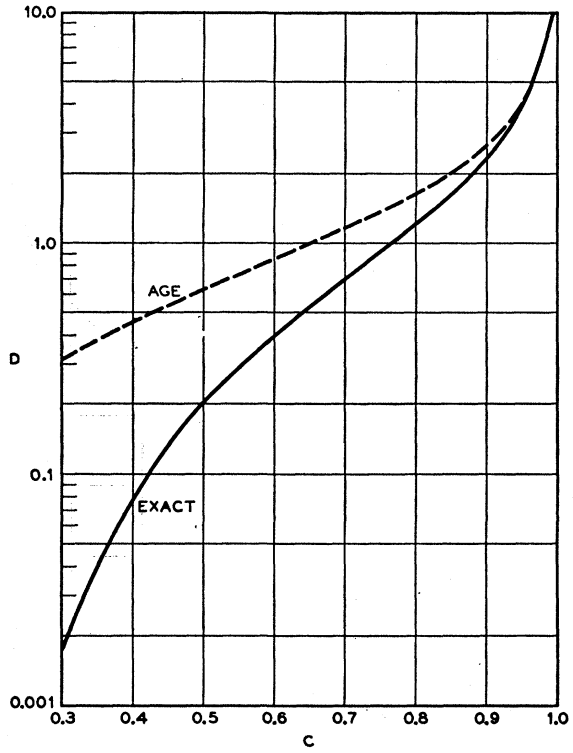

FIG. 6. The distribution constant D as a function of c.

Appendix B, but the results of that calculation, the six constants, are listed in Table III.

V. ANGULAR DEPENDENCE AND CURRENT

In this section, the angular dependence of the distribution function $g(z,U,\mu)$ will be calculated using the "last collision" method. The idea is that electrons leave their last (most recent before the observation) collision isotropically and proceed in straight line motion until they are observed as part of the distribution $g(z,U,\mu)$. Therefore, the number that are traveling in any given direction may be computed by counting the number of nearby collisions along a line in the direction of observation. Those electrons which are observed with energy loss U must have had, prior to the collision, an energy loss $U-\mathcal{E}_r$, and hence, the collision density $q(z', U-\mathcal{E}_r)$ is all that is needed to calculate $g(z,U,\mu)$.

Perhaps the easiest way to derive the last collision formula is to insert Eq. (3.8) into (3.6a) to obtain

$$[\mu(\partial/\partial z)+1]g(z,U,\mu)=c_0q(z,\,U-\mathcal{E}_r)+\delta(z)\delta(U)/l$$

and to integrate this equation, ignoring the source, to obtain

$$g(z,U,\mu)=\frac{c_0}{\mu}\int_{-\infty}^{z}q(z',\,U-\mathcal{E}_r)e^{-(z-z')/\mu}dz',\quad \mu\geq 0. \quad (5.1)$$

In ascribing physical meaning to (5.1), note that the factor c_0 is the probability that the electron actually survived the last collision and the exponential is the probability that the electron survived the transport from z' to z without intervening collision, a distance of $(z-z')/\mu$ mean free paths for an electron whose direction cosine with the z direction is μ. Hence, Eq. (5.1) is the last collision formula.

Suppose now that the medium is semi-infinite, terminating at $z=L$. Then the collision density to be used in (5.1) is the one appropriate to this bounded problem. If the boundary condition is complete emission, then the method of images may be used to construct a collision density which vanishes at $z=L'$, and (5.1) becomes

$$g(z,U,\mu)=\frac{c_0}{\mu}\int_{-\infty}^{z}[q(z',\,U-\mathcal{E}_r)-q(2L'-z',\,U-\mathcal{E}_r)]e^{-(z-z')/\mu}dz', \quad (5.2)$$

where the collision densities appearing in the integrand are the infinite medium solutions.

Because the infinite medium solution is not readily available, there is every reason for using the trial function approximation of Sec. II and Appendix C for the purpose of evaluating the integral. Recall that the z dependence of the trial function entered only through the parameters Q_0, $\bar{U}$, and δ^2, and recall that the dependence on Q_0 was multiplicative. Thus the trial function could have been written in the form

$$q_n(z,U)=Q_0(z)F[\bar{U}(z),\delta^2(z),U]. \quad (5.3)$$

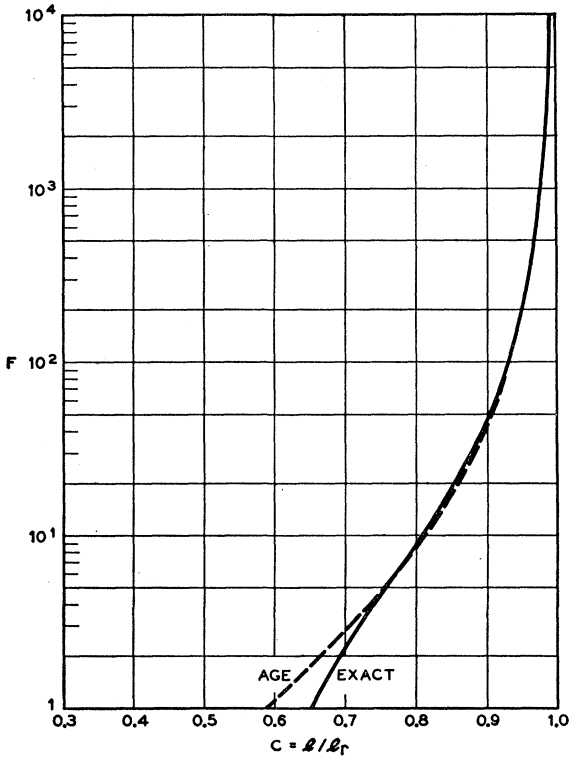

FIG. 7. The distribution constant F as a function of c.

Since the exponential in the integrand of Eq. (5.2) acts to limit the range of z' to a small neighborhood near z, it is appropriate to consider how the parameters Q_0, $\bar{U}$, and δ^2 vary over this limited range. Reference to Sec. IV and a guess at any reasonable values of c_0, $\mathcal{E}_r$, and z indicate that $\bar{U}$ and δ^2 are sluggish in their z dependence and hence, for the purpose of evaluating (5.2) they may be held fixed at their values at $z'=z$. That is, for the evaluation of (5.2), it is quite valid to set

$$q_n(z',U)=Q_0(z')F[\bar{U}(z'=z),\ \delta^2(z'=z),\ U]. \quad (5.4)$$

The parameter Q_0 had the form (Appendix C)

$$Q_0(z')=A\ \exp(-K_0z'), \quad (5.5)$$

where K_0 is the K of Eq. (4.1b) evaluated at $c=c_0$. Using (5.5) and (5.4) and (5.2) allows the integration to be performed. The result is

$$g(z,U,\mu)=c_0[(1-\mu K_0)^{-1}q(z,\ U-\mathcal{E}_r) -(1+\mu K_0)^{-1}q(2L'-z,\ U-\mathcal{E}_r)]. \quad (5.6)$$

Deep within the medium, the second term will be negligible in comparison to the first and the current,[12]

$$J(z,U)=\frac{l}{4\pi}\int_0^{2\pi}d\varphi\int_{-1}^{1}d\mu g(z,U,\mu)\mu, \quad (5.7)$$

will be

$$J=lc_0q(z,\ U-\mathcal{E}_r)K_0^{-2}[\tanh^{-1}K_0-K_0]$$

or, using (4.1b)

$$J=[(1-c_0)/K_0^2]q(z,\ U-\mathcal{E}_r)lK_0. \quad (5.8)$$

The approximation (5.4) indicates that $K_0q=-\partial q/\partial z$. Hence

$$J(z,U)=-\hat{D}\partial q(z,\ U-\mathcal{E}_r)/\partial z, \quad (5.9a)$$

$$\hat{D}=l[(1-c_0)/K_0^2]. \quad (5.9b)$$

The form of (5.9) is quite similar to the equation which relates g_0 to g_1 in the age approximation, or to Fick's law of diffusion which relates current to density gradient. Only under the conditions of validity of the age approximation, can one ignore the $\mathcal{E}_r$ energy difference between the two sides of (5.9a) and, because $c_0\approx 1$, give $\hat{D}$ its limiting value of $l/3$. This will, however, recover exactly the usual Fick's law of diffusion. Many of the results of the age approximation may be brought much closer to the exact solution merely by using (5.9) instead of the analogous equation in the bare age method.

The angular distribution at the edge of the medium is of interest. According to Ref. 8

$$L'=L+0.7104.$$

Hence, at the edge of the medium where $z=L$, Eq. (5.6)

[12] The factor of velocity inherent in the definition of current has, in Eq. (5.7) *et seq.* been absorbed in the $dp/dE=v^{-1}$ which converts the current per momentum dp to a current per energy dE.

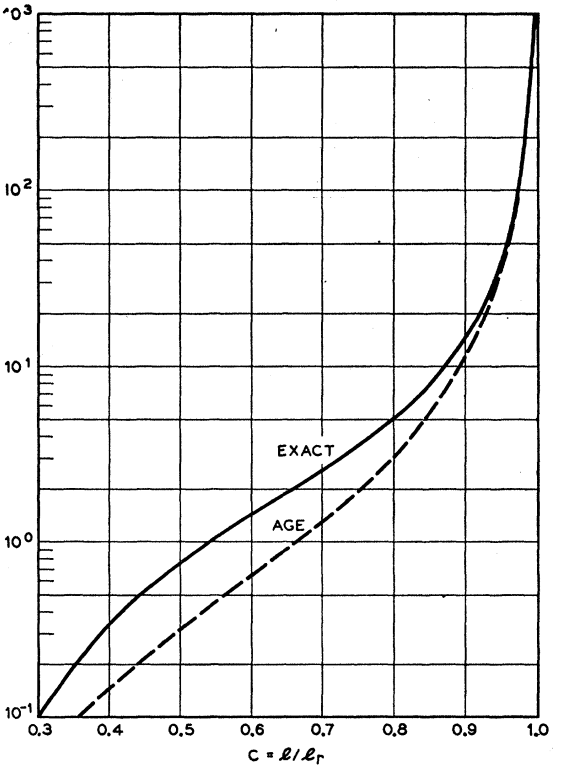

FIG. 8. The distribution constant G as a function of c.

may be evaluated, using (5.5) and (5.4) as

$$g(L,U,\mu)=c_0q(L,\ U-\mathcal{E}_r)f_K(\mu) \quad \mu>0, \quad (5.10a)$$

$$f_K(\mu)=(1-\mu K_0)^{-1}-(1+\mu K_0)^{-1} \times\exp(-1.4208K_0) \quad (5.10b)$$

as the angular distribution of outgoing particles just inside the boundary. The rate at which those particles whose trajectory lies within an angle $\theta_0=\cos^{-1}\mu_0$ of the normal will cross this boundary is

$$J(\mu_0)=\frac{l}{4\pi}\int_0^{2\pi}d\varphi\int_{\mu}^{1}d\mu g(z,U,\mu)\mu =lc_0q(L,\ U-\mathcal{E}_r)j_K(\mu_0), \quad (5.11a)$$

$$j_K(\mu_0)=\frac{1}{2K_0^2}\left[\ln\left(\frac{1-\mu_0K_0}{1-K_0}\right)-K_0(1-\mu_0)\right] -\frac{1}{2K_0^2}e^{-1.4208K_0}\left[\ln\left(\frac{1+\mu_0K_0}{1+K_0}\right)+K_0(1-\mu_0)\right]. \quad (5.11b)$$

Finally, there is one other boundary condition—this one of more relevance to the BMM experiment—which may be easily treated by the method of images. This is the condition that all electrons incident on the interface are reflected back into the medium. Assuming for sim-

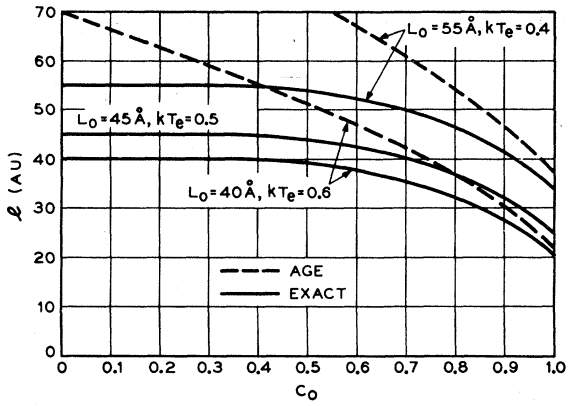

FIG. 9. Relationship between c_0 and l imposed by BMM measurement of L_0 and kT_e.

plicity that the vacuum-silicon interface acts as a perfect reflector, this means that

$$g(L,U,\mu)=g(L,U,-\mu). \tag{5.12}$$

To satisfy this boundary condition, one *adds* to the infinite medium solution with source at $z=0$ another infinite medium solution with source at $z=2L$. The effect of adding, rather than subtracting, is to change into a plus sign the minus sign separating the two collision densities in Eqs. (5.2), (6), (10b), and (11b). Putting the source at $2L$ deletes the exponential from these last two equations. Thus, under conditions of specular reflection at the boundary, the angular distribution at the boundary is

$$g(L,U,\mu)=c_0 q(L,U-\mathcal{E}_r)F_K(\mu), \tag{5.13a}$$

$$F_K(\mu)=(1-\mu K_0)^{-1}+(1+\mu K_0)^{-1}, \tag{5.13b}$$

while the rate at which electrons within the cone angle θ_0 impinge on the boundary is

$$J(\mu_0)=c_0 l q(L,U-\mathcal{E}_r)J_K(\mu_0), \tag{5.14a}$$

$$J_K(\mu_0)=\frac{1}{2K_0^2}\ln\left(\frac{1-K_0^2\mu_0^2}{1-K_0^2}\right). \tag{5.14b}$$

VI. INTERPRETATION OF THE BMM EXPERIMENTS

The BMM paper reports two experiments. In the first, the electrons were observed to be emitted in a distribution which had a temperature kT_e. By removing measured amounts of silicon from the path of the electrons and noting the resulting increase in current, BMM were able to obtain a value for the attenuation length L_0. The two quantities L_0 and kT_e impose, via Eq. (3.14) a relationship between c_0 and l which is plotted as Fig. 9. Each solid line in the figure corresponds to a different pair of values for the data. The central line corresponds to the values $L_0=45$ Å, $kT_e=0.5$ eV, which BMM take as their best determination. The other two lines correspond to the limits of error BMM set on their observations.

The dotted lines, shown for comparison, give the relation between c_0 and l which one would have inferred from the age approximation result, Eq. (3.18). The exact calculation gives a value of l which tends rapidly to the value L_0 as c_0 is decreased. This happens because, as the probability that the electron survives a collision drops well below unity, the only electrons which survive are those which do not collide at all. At large distance from the source, these travel directly away from the source and attenuate at a rate governed by the total mean free path—regardless of any considerations regarding the energy dependence of the distribution. Although the age approximation is asymptotic to the exact result as c_0 approaches unity, it leads one to expect values of l greater than the exact ones at all values of c_0. Therefore, we may expect that the BMM value for l will be larger than the true value, whatever c_0 turns out to be.[13,14]

The second BMM experiment was designed to supply a second relationship between l and c_0 so that c_0 and l can be determined uniquely. The experiment was a measurement of the spectral shape of the emerging electrons.

This second experiment is difficult to interpret because the spectral shape does depend on the details of the electric field in the junction, on the existence of a threshold energy below which ionization does not occur, on the energy dependence of the ionization cross section near the threshold and on the reflection of the electrons by the potential step as the silicon-vacuum interface. The troublesome part of the calculation of the spectral shape is the calculation of the source spectrum $S(E_0)$ whose parameters, S_0, $\langle E_0\rangle$, and δ_S^2 occur throughout Sec. II. Ideally, the Boltzmann equation should be solved without making the age approximation, but including the presence of a field, an ionization threshold and the behavior of the ionization cross section near threshold; this would be exceedingly difficult to do. There are, moreover, too many uncertainties in the actual field distribution and actual cross sections for us to even consider performing such a calculation at the present time. BMM have argued that the effect of all these uncertainties (and the effect of the age approximation itself) will be small. They may well be correct to so argue; we just cannot be certain.

We can be certain, however, that those electrons which are emitted must *maintain* a high energy while in the field-free region and that therefore, in that region, they never sample the cross sections near threshold. This means that a model which neglects the existence of the threshold region does apply to the field-free region.

[13] This tendency of the age approximation to overestimate the mean free path seems to be general. An example of this in a problem where there is an electric field may be constructed by comparing the results (Fig. 2) of Ref. 5 with those (Fig. 1) of Ref. 14.

[14] G. A. Baraff, Phys. Rev. **133**, A26 (1964).

One consequence of that model is, as we have seen, that *two* spectral measurements can determine the three constants B, D, G of Eq. (2.18) even without knowledge of the source spectrum or of the field distribution which produced it. If the two spectral measurements were to be made, then there would be absolutely no reason to attempt the calculation of the source spectrum or to worry about ionization thresholds.

Because the two spectral measurements are not yet available, it may be of some interest to assume that the various BMM arguments are correct and to try to learn what effect the age approximation alone has on the interpretation of the spectral shape measurement.

BMM found (using the age approximation) that the whole effect of diffusion through the neutral layer, a field-free region, may be included by considering the field region to be increased in width by the thickness of the neutral layer. This result may be considered from the converse point of view, that the whole effect of the field region preceding the neutral layer may be included by considering the neutral layer to be augmented in width by the thickness of the field region. The significant energy variable in this case is the energy loss U. Thus, the BMM finding means that the spectrum $M(x,E)$ may be calculated as though it were $q(x,E)$ with the result [Eq. (2.15)] that

$$M_0(x)=A\,\exp(-Bx/l)\,, \tag{6.1a}$$

$$\langle U(x)\rangle=\mathcal{E}_r(c+dX/l)\,, \tag{6.1b}$$

$$\delta_M{}^2(x)=\mathcal{E}_r{}^2(F+Gx/l)\,, \tag{6.1c}$$

with x being the distance from the *start* of the field region to the plane of observation. The results of this equation agree with the BMM results as given in BMM Fig. 2 when the constants A–G calculated by the age approximation are used.[15]

We are going to use Eq. (6.1), with the constants calculated exactly, as the description of the distribution to be compared with the BMM calculation. This is *not* the best possible description of the distribution at the end of the field-free region but it is the best we can do without recalculating the source distribution.

It seems very likely to us that the change in the distribution occasioned by using the exact constants in (6.1) rather than the age constants is a step in the right direction but one which does not go far enough.

The rough approximation just described for the treatment of the field region calls for a similar rough approximation for the treatment of the effect of the silicon-vacuum interface. At this interface, a potential step of energy ψ acts to keep electrons in the silicon. An electron whose energy is $\mathcal{E}_L$ will be reflected by this potential unless its trajectory lies within an angle θ_0 of the normal to barrier;

$$\cos\theta_0=\mu_0=(\psi/\mathcal{E}_L)^{1/2}. \tag{6.2}$$

The rough approximation is to assume that the cone angle θ_0 is small enough so that most of the electrons incident on the barrier will be reflected and that this reflection is elastic and specular. The distribution function near the barrier will then be given by Eq. (5.13) and the emitted current will be given by Eq. (5.14).

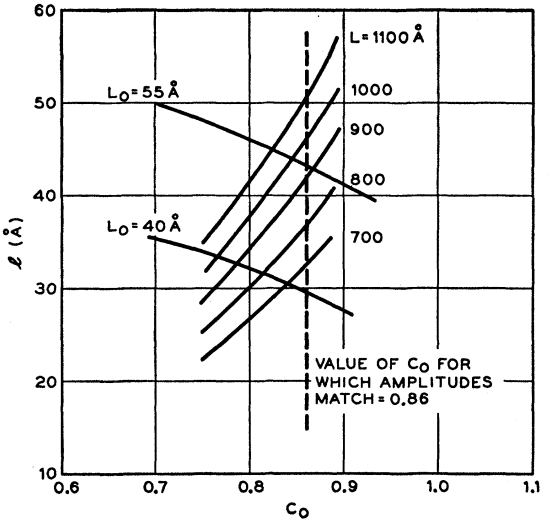

FIG. 10. Values of c_0 and l compatible with both BMM experiments.

The BMM data is the current of emitted electron as a function of electronic energy—i.e., the spectral shape of emitted electrons. Our expression (5.14) may be evaluated using the moments of Eq. (6.1) in the approximate inversion of Sec. II to provide a prediction of what that emitted spectrum should be. The spectrum calculated in this way depends on c_0 and on $z=L/l$ rather than on c_0 and on l directly. If L were known, this would be no problem, but, as BMM point out, the distance L is rendered uncertain precisely because of uncertainties about the field distribution and ionization threshold. All that we can do is to choose c_0 and z to fit the spectrum and to assign reasonable values to L so as to obtain the corresponding pair of values for c_0 and l which fit the spectrum.

The criterion we have chosen to measure the accuracy of the fit is the energy of the peak of the emitted distribution. Setting this energy (loss) at 1.5 eV (the observed value of the peak) gives, for each assignment of L, l as a function of c_0. Figure 10 depicts the family of l versus c_0 curves resulting. Each curve is labeled by the value of L assigned. A portion of Fig. 9 has been redrawn here, so that the l versus c_0 curves determined by the attenuation length L_0 appear superposed on those determined by fitting the peak of the distribution.

It turns out that the value $c_0=0.86$ fits the amplitude

[15] This comparison is made by using (6.1) for the parameters to calculate the peak of the distribution via Eq. (C1). x must be kept large enough to make the effect of C and F negligible. The converse of the BMM argument breaks down at small x because the field sweeps low-energy electrons away from the origin.

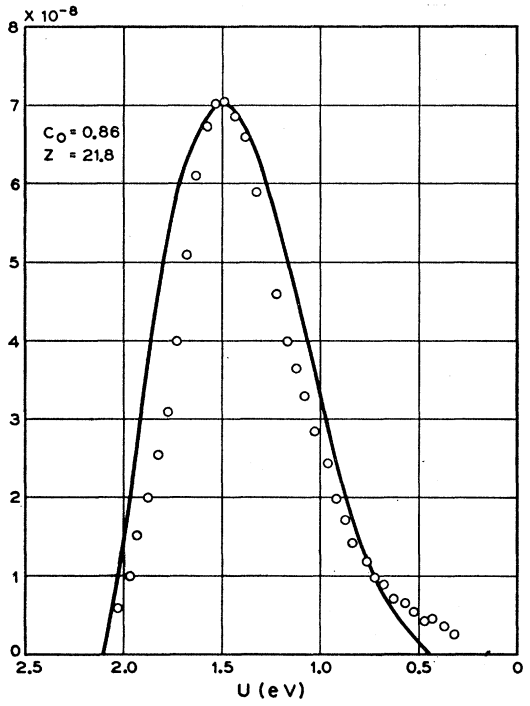

FIG. 11. Comparison of calculated and observed spectra.

of the peak. For the value of l corresponding, one has a range of choices consistent with the range of accuracy of the determination of L_0. On the one hand, one may assign a value to L (choosing perhaps the BMM guess of $L=900$ Å) and read off Fig. 10 the value of l corresponding (in this case $l=42$ Å) or one may assign a value to L_0 (choosing perhaps the BMM best estimate of $L_0=45$ Å) and read off Fig. 10 the value of l corresponding (in this case $l=34$ Å). The two spectrum measurement we have suggested would go far towards resolving the ambiguity here.

In Fig. 11, the spectrum calculated for $z=21.8$, $c_0=0.86$ is compared with the data from Bartelink's thesis.[16] This datum differs from that in BMM because the latter datum was arbitrarily shifted by 0.1 eV to fit the BMM theory. Any comments about the accuracy of fit between theory and experiment here would be premature if the two spectrum measurements are going to be made. It is our hope that they will soon be.

The tentative choice $l=38$ Å and $c_0=0.86$ leads to values

$$l_r=l/c_0=44\text{ Å}, \tag{6.3a}$$

$$l_i=l/(1-c_0)=270\text{ Å}, \tag{6.3b}$$

$$r=l_i/l_r=6.1. \tag{6.3c}$$

[16] D. J. Bartelink, Technical Report No. 1654-2, Solid State Electronics Laboratory, Stanford University, Stanford, California (unpublished).

ACKNOWLEDGMENTS

I should like to record a special indebtedness to Dr. Bartelink for the many long discussions we have had concerning the BMM paper and the present work. I should also like to acknowledge useful comments by Dr. C. R. Crowell, Dr. J. McKenna, and Dr. P. A. Wolff.

APPENDIX A: DIFFERENTIATION OF THE TRANSFORM

The asymptotic part of the solution given by Eq. (4.1) is

$$lq_s(z)=-(dK/dc)\exp(-Kz), \tag{A1a}$$

where

$$(K/c)=\tanh^{-1}K \tag{A1b}$$

and

$$c=c_0\exp(-S\mathcal{E}_r), \tag{A1c}$$

so that

$$(-d/dS)=c\mathcal{E}_r(d/dc). \tag{A2a}$$

It is useful to define

$$K_0=K(c_0)=c_0\tanh^{-1}K_0, \tag{A2b}$$

$$K_n\equiv(d/dc_0)^nK_0. \tag{A2c}$$

The differentiations (2.19) are easily performed and the result, suppressing the subscript zero on K_0 and c_0 are

$$lQ_0(z)=-K_1\exp(-Kz), \tag{A3a}$$

$$lQ_1(z)=-\mathcal{E}_rc(K_2-zK_1^2)\exp(-Kz), \tag{A3b}$$

$$lQ_2(z)=-\mathcal{E}_r^2(c^2K_1^3z^2-3zc^2K_1K_2 -zcK_1^2+cK_2+c^2K_3)\exp(-Kz). \tag{A3c}$$

Hence, using (2.13b) and (2.14b), the averages are

$$\langle U(z)\rangle=\mathcal{E}_rcK_2/K_1-\mathcal{E}_rcK_1z, \tag{A3d}$$

$$\delta_Q^2(z)=\mathcal{E}_r^2(c^2K_3/K_1+cK_2/K_1-c^2K_2^2/K_1^2) -\mathcal{E}_r^2(c^2K_2+cK_1)z. \tag{A3e}$$

Comparison of (A3) with (2.15) then gives

$$A=-K_1/l, \tag{A4a}$$

$$B=K_0, \tag{A4b}$$

$$C=c_0K_2/K_1, \tag{A4c}$$

$$D=-c_0K_1, \tag{A4d}$$

$$F=c_0^2K_3/K_1+c_0K_2/K_1-(c_0K_2/K_1)^2, \tag{A4e}$$

$$G=-c_0^2K_2-c_0K_1. \tag{A4f}$$

The derivatives K_n appearing here may be evaluated most readily by differentiating Eq. (A2b)

$$K_1=\frac{dK}{dc}=\frac{K(1-K^2)}{[c(1-K^2)-c^2]}, \tag{A5a}$$

TABLE IV. Derivatives of $K(c)$.

c	$-K_1$	$-K_2$	$-K_3$
0.2	0.0045	0.1805	5.216
0.3	0.0584	0.9396	8.159
0.4	0.1894	1.647	6.024
0.5	0.3822	2.200	5.434
0.6	0.6315	2.820	7.490
0.7	0.9594	3.850	14.37
0.8	1.444	6.220	38.62
0.9	2.400	15.48	212.8
0.92	2.761	21.10	369.4
0.94	3.276	31.69	753.1
0.96	4.120	56.81	2061
0.98	5.976	156.8	11 574
0.99	8.556	438.3	65 216

$$K_2=\frac{dK_1}{dc}=\frac{2c^2(1-c)K(1-K^2)}{[c(1-K^2)-c^2]^3}, \tag{A5b}$$

$$K_3=\frac{dK_2}{dc}=2c^3K(1-K^2)\times\frac{[3c(1-c)^2+4(1-c)K^2+(3c-4)K^4]}{[c(1-K^2)-c^2]^5}. \tag{A5c}$$

These derivatives are evaluated as functions of c_0 in Table IV.

APPENDIX B: AGE THEORY

Equation (3.6) governing $g(z,U,\mu)$ may be treated within the framework of the age theory approximation. One writes

$$g(z,U,\mu)=g_0(z,U)+\mu g(z,U), \tag{B1a}$$

$$g(z,\,U-\mathcal{E}_r,\,\mu)=g(z,U,\mu)-\mathcal{E}_r\partial g/\partial U. \tag{B1b}$$

Insert (B1) into (3.6) and then

(a) Integrate the result over μ.

(b) Multiply the result by μ and then integrate over μ.

A pair of coupled equations result and these may be combined into the single equation for g_0, namely

$$\left[\frac{1}{3}\frac{\partial^2}{\partial z^2}-(1-c_0)-c_0\mathcal{E}_r\frac{\partial}{\partial U}\right]g_0(z,U)+\frac{\delta(z)\delta(U)}{l}=0. \tag{B2}$$

The Laplace transform of (B2) with respect to U is

$$\left[\frac{1}{3}\frac{d^2}{dz^2}-(1-c_0+c_0\mathcal{E}_rs)\right]g_s(z)+\frac{\delta(z)}{l}=0, \tag{B3a}$$

$$g_s(z)=\int_0^\infty g_0(z,U)\exp(-sU)dU, \tag{B3b}$$

and the solution is

$$g_s(z)=(3/2Kl)\exp(-K|z|), \tag{B4a}$$

$$K^2=3[1-c(s)], \tag{B4b}$$

$$c(s)=c_0(1-s\mathcal{E}_r). \tag{B4c}$$

Applying the age approximation to (3.8) shows that $g_0(z,U)$ is itself the collision density. Hence, the transform $q_s(z)$ is

$$q_s(z)=g_s(z)=(3/2Kl)\exp(-Kz). \tag{B5}$$

This is the function which yields the attenuation length by setting $s=1/kT_e$, and the moments by the differentiation indicated by Eq. (2.19). The attenuation length L_0 is given by

$$L_0^2=l^2/K^2=l^2/3[1-c(1/kT_e)], \quad =ll_i/3[1+r\mathcal{E}_r/kT_e], \tag{B6}$$

which is identical to Eq. (3.18). In performing the differentiations, the observation that the only s dependence enters (B5) through K leads to

$$\frac{d}{ds}=\frac{dK}{ds}\frac{d}{dK}=\left(\frac{3c_0\mathcal{E}_r}{2K}\right)\frac{d}{dK}.$$

Hence, the results of the differentiation and algebra are

$$Q_0(z)=(3/2lK_0)\exp(-K_0z), \tag{B7a}$$

$$Q_1(z)=(9c\mathcal{E}_r/4lK_0)(K_0^{-2}+zK_0^{-1})\exp(-K_0z), \tag{B7b}$$

$$Q_2(z)=(27c^2\mathcal{E}_r^2/8lK_0)(3K_0^{-4}+3K_0^{-3}z+K_0^{-2}z^2)\times\exp(-K_0z), \tag{B7c}$$

$$K_0^2=3(1-c_0), \tag{B7d}$$

and the parameters are

$$\langle U(z)\rangle=[c_0\mathcal{E}_r/2(1-c_0)](1+K_0z), \quad \delta_Q^2(z)=[c_0\mathcal{E}_r/2(1-c_0)]^2(2+K_0z). \tag{B8a}$$

Comparison of Eqs. (B7), (B8) with Eq. (2.20) yields

$$lA=[3/4(1-c_0)]^{1/2}, \tag{B9a}$$

$$B=[3(1-c_0)]^{1/2}, \tag{B9b}$$

$$C=c_0/2(1-c_0), \tag{B9c}$$

$$D=[3c_0^2/4(1-c_0)]^{1/2}, \tag{B9d}$$

$$F=[c_0/(1-c_0)]^2/2, \tag{B9e}$$

$$G=[3c_0^4/16(1-c_0)^3]^{1/2}. \tag{B9f}$$

The numerical evaluation of (B9) is given in Table III and Figs. 2–7.

APPENDIX C: AN APPROXIMATE INVERSION

The fact that the shape of the trial function Eq. (2.20) is fairly insensitive to the value of n chosen may be demonstrated most easily by calculating the energy and magnitude of the peak of the distribution. The maximum value of $q_n(z,U)$ occurs at

$$U_{\max}=U_0+n/\gamma$$

and the value of q at its maximum is

$$q_n(z,U_{\max})=Q_0[(n+1)/n\delta^2]^{1/2}g_n,$$
$$g_n\equiv n^{n+\frac{1}{2}}e^{-n}/n!.$$

However, using (2.22), one has

$$U_{\max}=\bar{U}-[\delta^2/(n+1)]^{1/2} \tag{C1}$$

and using Stirling's formula for the factorial,[17] one has very nearly

$$q_n(z,U_{\max})=Q_0[(n+1)/(2\pi n\delta^2)]^{1/2}. \tag{C2}$$

The position and amplitude of the peak, two quantities which *do* depend on the shape of the trial function, are exhibited in Eqs. (C1), (C2). The fact that for $n>2$, they are very weakly dependent on n is an example of the way the quantitative information acts to restrict the variation of the trial function.

The considerations leading to the choice of n are the following: the trial function (2.20) has been adjusted so as to approximate the collision density $q(z,U)$. Hence, the Laplace transform of the trial function should approximate the Laplace transform of the collision density, $q_s(z)$. *If* the approximation were exact, one would have

$$q_s(z)=\int_0^\infty q_n(z,U)e^{-sU}dU$$
$$=[an!/(\gamma+s)^{n+1}]\exp(-sU_0), \tag{C3}$$

and equality for *all* values of s. The approximation is not exact however and thus (C3) is not true for all values of s. (Even so, when both sides of this equation are expanded as power series in s, there *is* agreement up to terms in s^2 because of the choice of α, U_0, and γ.) We may express α, γ, and U_0 in terms of Q_0, $\bar{U}$, and δ^2 using Eq. (2.22). Then a slight rearrangement of (C3) gives

$$[Q_0(z)/q_s(z)]\exp(-s\bar{U})$$
$$=\{1+s[\delta^2/(n+1)]^{1/2}\}^{n+1}e^{-s[(n+1)\delta^2]^{1/2}}. \tag{C4}$$

The only value of s important to the inversion of (C3) is evidently $s=-\gamma$. One would prefer to choose n so that (C4) is indeed an equality for this single value of s. This is not possible, but by choosing another nearby value of s, namely

$$s=-\gamma/(n+1)^{1/2}=-1/\delta, \tag{C5}$$

it is possible to choose n so as to satisfy (C4) at this one value of s. Doing this will cause the transform and its approximant not only to agree at the origin up to terms of order s^2, but to agree again at a value of s near the region which should be important to the process of inverting the transform.

To achieve this, one may insert (C5) into (C4) to obtain

$$[Q_0(z)/q_{-1/\delta}(z)]\exp(\bar{U}/\delta)=f_n, \tag{C6a}$$

$$f_n=[1-(n+1)^{-1/2}]^{n+1}\exp(n+1)^{1/2}. \tag{C6b}$$

The left side of (C6a) is an easily calculated function of z. The new symbol $q_{-1/\delta}$ indicates that $q_s(z)$ is to be calculated with s set equal to $-1/\delta$. The right side of (C6a) is a function of n which may be tabulated once and for all for integer values of n (see Table V). The value of n to be used in (2.20), (2.22) and (C1), (C2) is that integer which best satisfies Eq. (C6).

TABLE V. The function f_n.

n	f_n	n	f_n
1	0.3528	11	0.5361
2	0.4267	12	0.5394
3	0.4618	13	0.5423
4	0.4829	14	0.5449
5	0.4473	15	0.5472
6	0.5079	16	0.5493
7	0.5160	17	0.5511
8	0.5225	18	0.5529
9	0.5278	19	0.5544
10	0.5323	20	0.5559

Although we do not know how to invert the exact $q_s(z)$ we do know how to invert the corresponding function, namely Eq. (B5), in the age approximation. The inversion is

$$lq(x,U)=[3/(4\pi c_0\mathcal{E}_rU)]^{1/2}$$
$$\times\exp\{-[(3c_0\mathcal{E}_rz^2/4U)+(1-c_0)U/c_0\mathcal{E}_r]\} \tag{C7}$$

in full agreement with the results of BMM. This inversion appears as the solid curve of Fig. 1 which corresponds to the choice $z=22$, $c_0=0.76$, $\mathcal{E}_r=0.063$ eV. The points lying just above or below the curve were calculated using the trial function method as described in Sec. II, and the age approximation for computing the moments.

[17] The formula states that $\lim_{n\to\infty} g_n=(2\pi)^{-1/2}$. However, for $n\geq 2$, the difference between g_n and its limiting value is already less than 4%. See, for example, Ref. 8, p. 443.